A transitional period of Ca^{2+}-dependent spike afterdepolarization and bursting in developing rat CA1 pyramidal cells

Shmuel Chen, Cuiyong Yue and Yoel Yaari

Department of Physiology, Institute of Medical Sciences, Hebrew University School of Medicine, Jerusalem 91120, Israel

During postnatal development neurones display discharge behaviours that are not present in the adult, yet they are essential for the normal maturation of the nervous system. Neonatal CA1 pyramidal cells, like their adult counterparts, fire regularly, but excitatory GABAergic transmission drives them to generate spontaneous high-frequency bursts until postnatal day (P) 15. Using intracellular recordings in hippocampal slices from rats at P8 to P25, we show herein that as the network-driven burst activity fades out, most CA1 pyramidal cells become intrinsically bursting neurones. The incidence of intrinsic bursters begins to rise at P11 and attains a peak of 74% by P18–P19, after which it decreases over the course of a week, disappearing almost entirely at P25. Analysis of the effects of different voltage-gated Ca^{2+} and Na^{+} channel antagonists, applied focally to proximal and distal parts of developing neurones, revealed a complex burst mechanism. Intrinsic bursting in developing neurones results from 'ping-pong' interplay between a back-propagating spike that activates T/R- and L-type voltage-gated Ca^{2+} channels in the distal apical dendrites and persistent voltage-gated Na^{+} channels in the somatic region. Thus, developing pyramidal neurones transitionally express not only distinctive synaptic properties, but also unique intrinsic firing patterns, that may contribute to the ongoing formation and refinement of synaptic connections.

(Received 10 February 2005; accepted after revision 23 May 2005; first published online 26 May 2005)
Corresponding author Y. Yaari: Department of Physiology, Hebrew University School of Medicine, PO Box 12272, Jerusalem 91120, Israel. Email: yaari@md2.huji.ac.il

Although the capacity of CNS neurones to generate propagating action potentials appears already *in utero* (Spitzer & Ribera, 1998), their distinctive adult firing patterns are elaborated after birth (Spitzer *et al.* 2002). The postnatal maturation of intrinsic excitability accompanies and interacts with other developmental programmes that underlie neuronal growth, ramification of axonal and dendritic branches and formation and pruning of synaptic connections. During this period neurones display patterns of collective firing that are not ordinarily manifested by their mature counterparts. Yet, these immature patterns may be fine-tuned to carry out certain vital developmental functions (Moody, 1998). Identifying the transitional patterns of neuronal activity and their underlying intrinsic and synaptic mechanisms is therefore essential for understanding CNS development.

Adult hippocampal CA1 pyramidal cells normally fire a single spike when depolarized by a brief stimulus. In response to sustained stimuli they fire a train of spikes which adapts partially or completely (Schwartzkroin, 1975; Madison & Nicoll, 1984). Neonatal CA1 pyramidal cells fire in a similar mode, though they are less excitable than the mature neurones (Schwartzkroin & Kunkel, 1982; Costa *et al.* 1991). During the first 3–4 postnatal weeks their intrinsic excitability progressively increases. In this period action potentials become faster and larger. Likewise, the spike afterdepolarization (ADP) becomes progressively longer. However, it was noted that despite the monotonic changes in these measures of intrinsic excitability, many neurones temporarily manifest a tendency to burst fire during their maturation (Costa *et al.* 1991).

In this study we have investigated in detail developmental changes in the firing modes of CA1 pyramidal cells. We report that between P12 and P19, up to 74% of the neurones convert to a bursting mode after which (between P20 and P25) they rapidly revert to the adult pattern of regular firing. Moreover, we show that bursting in this transitional period results from 'ping-pong' interplay between a back-propagating spike that activates specific subtypes of voltage-gated Ca^{2+} channels in the apical dendrites and persistent Na^{+} channels in the somatic region. We discuss the possibility

 DOI: 10.1113/jphysiol.2005.084590

that this transitional mode of bursting may be important for the refinement of synaptic connections in developing hippocampal neurones.

Methods

Slice preparation

Transverse hippocampal slices were prepared from young (P8–P25) and adult (> P30) male Sabra rats. Animals were decapitated under isoflurane anaesthesia, and transverse hippocampal slices (400 μm) were prepared with a vibrating microslicer (Leica) and transferred to a storage chamber perfused with oxygenated (95% O_2–5% CO_2) artificial cerebrospinal fluid (ACSF) containing (mM): NaCl 124, KCl 3.5, $MgCl_2$ 2, $CaCl_2$ 1.6, $NaHCO_3$ 26 and D-glucose 10; pH 7.4, osmolarity 305 mosm l^{-1}, where they were maintained at room temperature (20–22°C). For experiments, slices were placed one at a time in an interface chamber (33.5°C) and perfused with oxygenated ACSF. The slices were positioned so that their antero-posterior axis was in the direction of ACSF flow. When 0.5 mM $NiCl_2$ was added to the ACSF, the amount of $MgCl_2$ was reduced to 1.5 mM to maintain an equal concentration of divalent cations. In some experiments the ACSF also contained the glutamate receptor antagonists 6-cyano-7-nitro-quinoxaline-2,3-dione (CNQX; 15 μM) and 2-amino-5-phosphono-valeric acid (APV; 50 μM) to block fast excitatory postsynaptic potentials, and the $GABA_A$ receptor antagonist bicuculline (10 μM) to block fast inhibitory postsynaptic potentials.

Electrophysiological methods

Intracellular recordings were obtained using sharp glass microelectrodes containing 4 M potassium acetate (90–110 MΩ). An active bridge circuit in the amplifier (Axoclamp 2A, Axon Instruments, Union City, CA, USA) allowed simultaneous injection of current and measurement of membrane potential. The bridge balance was carefully monitored and adjusted before each measurement. The pyramidal cells included in this study had stable resting potentials of at least −60 mV and overshooting action potentials. In some experiments, bipolar platinum (50 μm) electrodes connected to a stimulator (Master8, AMPI, Jerusalem, Israel) by an isolation unit were used for focal stimulation of afferent fibres in stratum radiatum near the CA2–CA3 border (orthodromic stimulation). The intracellular signals were digitized and stored on a personal computer using a data acquisition system (Digidata 1322A) and pCLAMP software (Axon Instruments).

For focal drug applications we used a puffing system consisting of a pneumatic pump (Picospritzer III, General Valve, Fairfield, NJ, USA) connected to a patch pipette filled with ACSF and the drugs to be focally applied. The tip of the pipette touched the upper surface of the slice. The amplitude and duration of pressure pulses used for puffing drugs (typically 5 bar and 20 ms, respectively) were set to produce a drop that initially covered a circular area ~50 μm in diameter on the surface of the slice, as tested by including 0.2% fast-green dye in the puffing pipette. The experimental arrangement is shown in Fig. 1*A*. For somatic drug application, the puffing pipette was positioned in stratum pyramidale about 25 μm from the recording microelectrode (lodged in the soma of the neurone) and upstream with respect to the direction of ACSF flow. To apply drugs to the distal apical dendrites, the puffing pipette was positioned in stratum radiatum about 200–300 μm away from, and vertical to, the stratum pyramidale. In a series of control experiments ($n = 5$) we found that one drop of 0.5 μM tetrodotoxin (TTX) applied to the soma, increased spike threshold (tested with 4-ms depolarizing current pulses) within 1–3 min and blocked somatic spiking within 5 min. Likewise, one drop of 5 mM Ni^{2+} suppressed the Ca^{2+}-dependent slow afterhyperpolarization (sAHP) that is generated at the soma following a train of spikes (Madison & Nicoll, 1984; Bowden *et al.* 2001) within 3–5 min ($n = 6$; see below, Fig. 1*Ca* and *b*, bottom traces).

To assess the efficacy of focal drug applications to the apical dendrites, we tested the effects of TTX and Ni^{2+} (same concentrations as above) on bursting induced by 4-aminopyridine (4-AP). It is known that exposing CA1 pyramidal cells to millimolar concentrations of 4-AP, by blocking A-type K^+ current (I_A), facilitates spike back-propagation and activation of dendritic Ca^{2+} channels (Hoffman *et al.* 1997; Magee & Carruth, 1999). The resultant dendritic Ca^{2+} spike spreads back to the soma and triggers two to three additional spikes. Consequently, 4-AP-induced bursts can be blocked by distal applications of either TTX (which blocks Na^+ spike backpropagation) or Ni^{2+} (which blocks the Ca^{2+} spike). In both cases the initiating somatic spike would be unaffected, provided the drugs do not spread to the somatic region. To deliver the drugs to a large portion of the apical dendrites, we applied three drops in immediate succession for each drug test. Representative results are shown in Fig. 1*B* and *C*. Bath applied 4-AP induced somatic bursts of three to four spikes in all experiments (Fig. *Ba* and *b*). Puffing TTX onto the apical dendrites blocked all but the first spike within 3 min (Fig. 1*Bc*; $n = 4$). The rise time and amplitude of the first spike were not affected even 10 min after TTX application, indicating that TTX did not reach the soma. Puffing Ni^{2+} onto the soma (one puff; 5 mM Ni^{2+} in the application pipette) did not affect bursting (Fig. 1*Ca* and *b*, top traces) though it suppressed the sAHP (Fig. 1*Ca* and *b*, bottom traces), but after moving the application pipette to the dendritic location, Ni^{2+} application (three puffs) blocked the burst within 4–6 min (Fig. 1*Cc*; $n = 3$).

Together, these results show that focally applied drugs reach their targets and do not spread appreciably from soma to apical dendrites and vice versa. We found that to replicate effects of bath applied drugs, the optimal drug concentrations in our puffing pipettes should be tenfold higher than those used in bath applications. Effects of puffed drugs, when present, were usually observed within 3 min after puffing and monitored for 10–15 min.

Chemicals

All chemicals and drugs were obtained from Sigma (Petach-Tikva, Israel), apart from ω-conotoxin MVIIC, apamin, calciseptine (Alomone Laboratories, Jerusalem, Israel) and CNQX (RBI, Natick, MA, USA). Stock solutions of nimodipine (10 mM) and BAY-K8644 (1 mM) were prepared in dimethyl sulfoxide (DMSO) and diluted 1 : 1000 when added to the ACSF. In experiments testing the effects of the latter two drugs, equivalent amounts of DMSO were added to the control ACSF. All other drugs were added to the ACSF from aqueous stock solutions.

Data analysis

The intensity of bursting was quantified only from responses to brief (4 ms), threshold-straddling depolarizing current pulses. Two variables were measured, namely, the number of intraburst spikes (N_s) and the duration of the spike ADP. The latter variable was measured as the interval between two points: the time of the fast AHP (fAHP) following the first spike and the time taken for the ADP to decay to 50% of its initial amplitude (at the first time point). Assessment of statistical significance of differences between means was performed with one- way ANOVA or paired Student's *t* test, as appropriate. Significance of linear regression models was tested using *t* statistics. The *t* statistics were used to test whether slope coefficients of linear regression lines were significantly different from zero. In all tests significance level was set to $P < 0.05$.

Results

Intrinsic bursting in developing pyramidal cells

In this study, we have investigated with sharp intracellular microelectrodes the intrinsic firing patterns of 215 developing (P8–P25) and 38 adult (P30–P50) rat CA1 pyramidal cells in acute hippocampal slices perfused with normal ACSF. When depolarized with brief (4 ms) depolarizing current pulses, some neurones fired a single spike, whereas others fired a high-frequency (163.8 ± 38.2 Hz; $n = 30$) burst of two or more spikes as their minimal response (Fig. 2*A*). According to the number

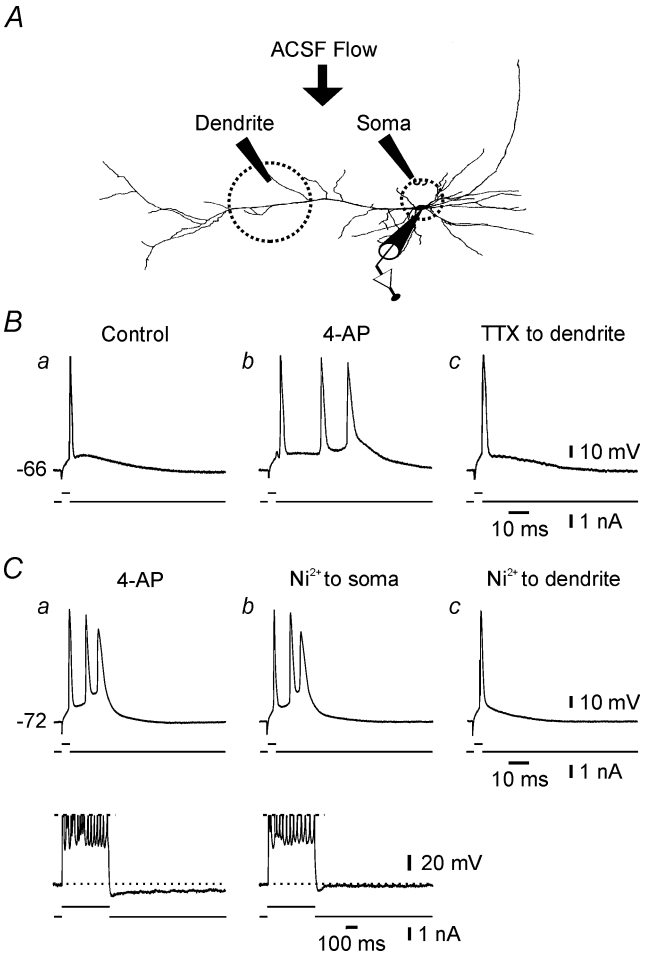

Figure 1. Experimental arrangement for focal drug applications to CA1 pyramidal cells
A, scheme of experimental arrangement. For somatic drug application, the puffing pipette was positioned in stratum pyramidale about 25 μm from the recording microelectrode (lodged in the soma of the neurone) and upstream with respect to the direction of ACSF flow. To apply drugs to the distal apical dendrites, the puffing pipette was positioned in stratum radiatum about 200–300 μm away from, and vertical to, the stratum pyramidale. *B*, effects of puffing TTX on the apical dendrites on 4-AP-induced bursting. In this and in the following figures, the lower trace represents the current stimulus and the upper trace is the voltage response. The resting potential is indicated to the left of the voltage trace. In normal ACSF, the neurone fired solitary spikes when stimulated with 4 ms depolarizing current pulses (*a*). Adding 3 mM 4-AP to the ACSF enhanced the spike ADPs so that after ~15 min the neurone fired bursts of three spikes in response to the same stimuli (*b*). Distal application of TTX (three puffs) suppressed the two late spikes of the burst within 3 min, without affecting the primary spike (c). *C*, effects of focal applications of Ni^{2+} on 4-AP-induced bursting. In this neurone also adding 3 mM 4-AP to the ACSF induced bursting. Proximal application of Ni^{2+} (one puff) did not modify the burst response (*a* and *b*, top traces), but markedly suppressed the sAHP evoked by 500-ms depolarizing current pulses (*a* and *b*, bottom traces). After the same application pipette was moved distally, application of Ni^{2+} to the apical dendrites (three puffs) suppressed the burst within 5 min.

of spikes evoked by brief stimuli (N_S), these neurones were classified into two groups, namely, non-bursters (i.e. $N_S \geq 1$) and bursters (i.e. $N_S = 2$). Bursting behaviour was unaffected by blocking fast excitatory and inhibitory synaptic transmission with 15 μM CNQX, 50 μM APV and 10 μM bicuculline ($n = 10$), confirming its intrinsic nature.

The proportion of bursting pyramidal cells was strongly dependent on postnatal age. This relationship is plotted in Fig. 2*B*. In this plot, each point represents the data

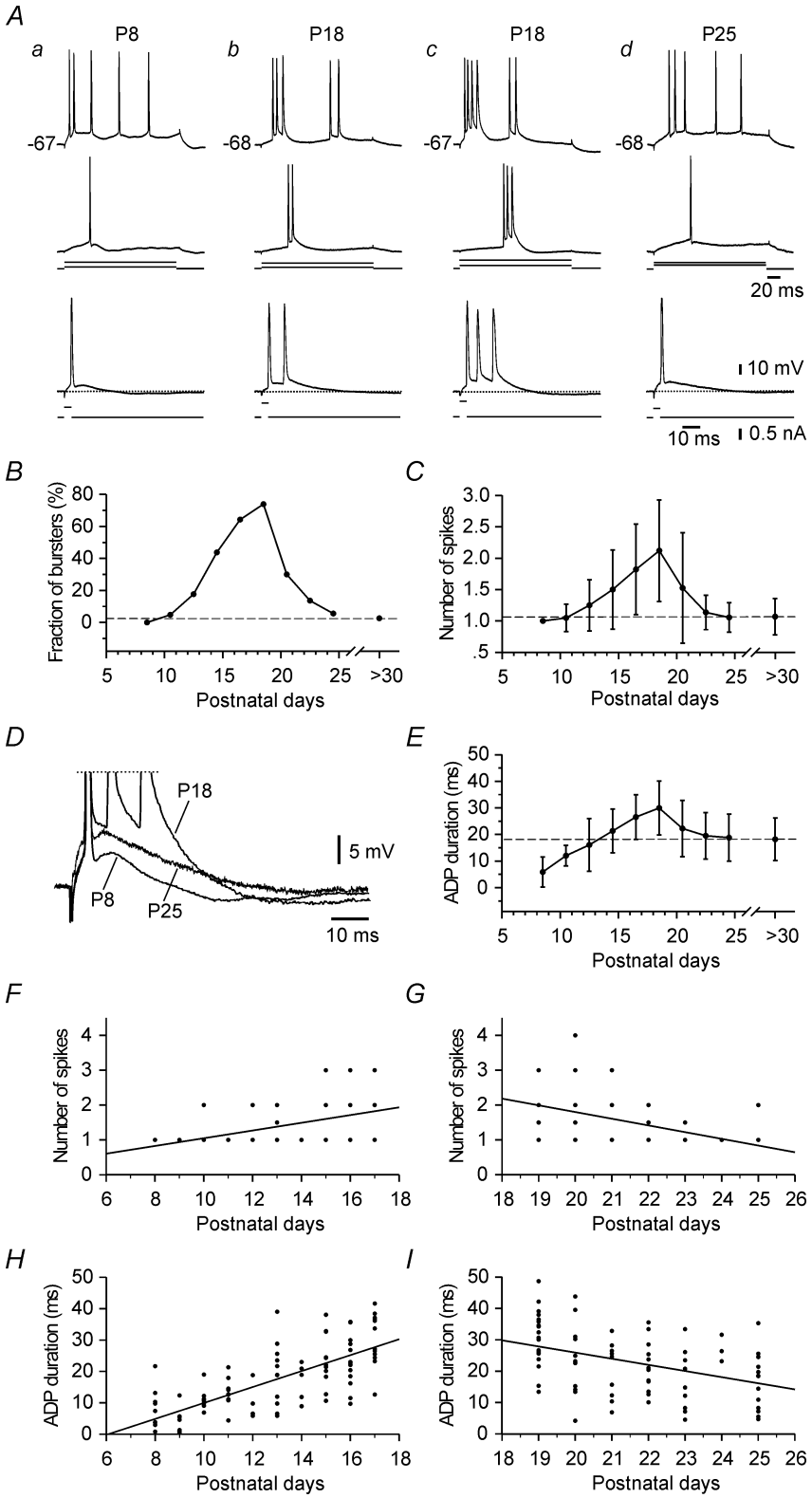

Figure 2. Developmental changes in firing patterns and spike ADPs in CA1 pyramidal cells
A, the intrinsic firing patterns of four representative neurones recorded in slices from P8 (*a*), P18 (*b* and *c*) and P25 (*d*) rats. Both P8 (*a*) and P25 neurones (*d*) fire in a regular pattern when stimulated with long (180 ms) depolarizing current pulses and generate only one spike in response to brief (4 ms) stimuli. The P18 neurones (*b* and *c*) generate bursts in response to similar stimuli. *B*, plot of the fraction of bursting CA1 pyramidal cells *versus* postnatal age. Each point represents the fraction of bursters in a sample of at least 20 neurones recorded on two sequential days from P8 to P25 rats (P8–P9, P10–P11, etc.). The point representing adult (> P30) neurones describes the fraction of bursters in 38 neurones from P30 to P50 rats. The dashed line represents the fraction of bursters in the adult neurones. *C*, plot of the mean number (± S.D.) of spikes evoked by brief stimuli *versus* postnatal age. The data are taken from the same neurones described in *A*. The dashed line represents the mean N_S in adult neurones. *D*, representative spike ADPs from P8, P18 and P25 neurones shown in *Aa* cand *d*. The traces are overlaid to facilitate comparison of ADP size. *E*, plot of spike ADP durations (mean ± S.D.) *versus* postnatal age. The dashed line represents the spike ADP duration in adult neurones. *F*, trend analyses of changes in N_S from P8 to P17. The line through the data points was obtained by linear regression analysis and has a slope coefficient of 0.11. *G*, same as *F*, but for P19 to P25, yielding a slope coefficient of −0.19. *H*, trend analyses of changes in spike ADP duration from P8 to P17. The line through the data points was obtained by linear regression analysis and has a slope coefficient of 2.53. *I*, same as *H*, but for P19 to P25, yielding a slope coefficient of −1.96. ADP, afterdepolarization; N_S, number of intraburst spikes; S.D., standard deviation.

obtained from at least 20 neurones at two sequential postnatal days. Between P8 and P11 practically all neurones examined (98%; 39 of 40 neurones) were non-bursters (Fig. 2*Aa*). During the following week the incidence of bursters increased dramatically, attaining a peak of 74% (34 of 46 neurones) at P18–P19 (Fig. 2*Ab* and *c*). However, within the subsequent week the incidence of bursters decreased sharply, returning to 7% (1 of 15 neurones) by P25 (Fig. 2*Ad*). By comparison, the incidence of bursters in adult CA1 pyramidal cells was 3% (1 of 38 neurones). As expected, the relationship between the mean N_S values in developing neurones *versus* their postnatal age also indicated a transitional increase peaking at P18–P19 (Fig. 2*C*).

In adult CA1 pyramidal cells, fast spike repolarization is incomplete, and is followed by a prominent spike ADP (Schwartzkroin, 1975; Jensen *et al.* 1994). We have previously shown that the propensity to generate intrinsic bursts is correlated with relatively large and prolonged ADPs, which serve as the generator potentials of the burst responses (Jensen *et al.* 1994, 1996). Therefore, we also compared the duration of spike ADPs (see Methods) at different postnatal days. Representative recordings of ADPs from P8, P18 and P25 neurones are overlaid in Fig. 2*D* and the averaged data are plotted in Fig. 2*E*. The spike ADPs in the youngest age group (P8–P9) were brief. They increased considerably within the subsequent week, attaining maximal duration at P18–P19, the time of maximal bursting. After this peak, spike ADP durations decreased partially, attaining adult values at P24–P25. At this age, as in adult neurones, the spike ADPs were about 3-fold longer than in the youngest age group (Fig. 2*D*), but not sufficiently large to trigger bursting in most of the neurones.

Despite the large variance in N_S and in spike ADP duration across neurones of the same postnatal age (Fig. 2*C* and *E*), the developmental changes in these intrinsic properties were statistically significant. In order to further evaluate the significance of the gradual increases (between P8 and P17) and decreases (between P19 and P25) in N_S and spike ADP duration, we performed trend analysis on the data obtained before and after P18. The data for P8–P17 and P19–P25 are plotted in Fig. 2*F* and *H* and Fig. 2*G* and *I*, respectively, and the solid lines represent linear regression fits through all data points. In all four cases the linear regression model was significant. The slope coefficients obtained for the fitted regression lines were positive for P8–P17 and negative for P19–P25 and in all cases significantly different from zero. The results of these analyses corroborate our conclusion that a transitional increase in burst firing due to augmented spike ADP takes place in CA1 pyramidal cells between P8 and P25.

Effects of blocking voltage-gated Ca^{2+} channels

Although adult CA1 pyramidal cells in hippocampal slices do not normally manifest bursting activity, they can be induced to do so by various acute manipulations, such as raising the concentration of K^+ in the ACSF or blocking certain K^+ conductances (Jensen *et al.* 1994, 1996; Azouz *et al.* 1996; Magee & Carruth, 1999; Su *et al.* 2001; Yue & Yaari, 2004). Two distinct ionic mechanisms have been proposed to account for bursting in these neurones. One mechanism involves recruitment of voltage-gated Ca^{2+} channels in apical dendrites by the back-propagating somatic spike; the ensuing Ca^{2+} current (I_{Ca}) then generates a slow dendritic Ca^{2+} spike that reinforces the somatic spike ADP, leading to repetitive discharge (Magee & Carruth, 1999). The other mechanism involves the activation of a persistent Na^+ current (I_{NaP}) at or near the soma, which regeneratively augments the somatic spike ADP beyond the threshold for bursting (Azouz *et al.* 1996; Su *et al.* 2001). Clearly, these mechanisms are not mutually exclusive and may act synergistically to generate bursting behaviour. To assess the involvement of voltage-gated Ca^{2+} channels in burst generation in developing CA1 pyramidal cells, we first examined the effects of the Ca^{2+} channel blocker Ni^{2+} on this activity. At a concentration of 0.5 mM that does not discriminate between different types of Ca^{2+} channels, Ni^{2+} completely suppressed bursting (from 2.1 ± 0.3 to 1.0 ± 0.0 spikes, $n = 7$; Fig. 3*A*) and markedly reduced the spike ADP duration in all neurones tested (from 30.4 ± 7.3 to 10.1 ± 1.7 ms; $P < 0.05$).

Because millimolar concentrations of Ni^{2+} may also reduce Na^+ currents (Jung *et al.* 2001), we conducted similar experiments using a mixture of type-selective Ca^{2+} channel blockers previously found to totally inhibit I_{Ca} in CA1 pyramidal cells (Su *et al.* 2002). In these experiments the modified ACSF contained 0.1 mM Ni^{2+}, 10 μM nimodipine and 5 μM ω-conotoxin MVIIC (CTX) to block T/R-, L- and N/P/Q-types of Ca^{2+} channels, respectively (McCarthy & TanPiengco, 1992; Catteral, 2000). As illustrated in Fig. 3*B*, application of these drugs completely suppressed bursting (from 2.5 ± 0.5 to 1.0 ± 0.0 spikes; $n = 8$), while markedly reducing the spike ADP duration in all neurones tested (from 31.1 ± 5.8 to 10.8 ± 2.1 ms; $P < 0.05$).

The results of the above experiments are summarized in Fig. 3*C* and *D*. They suggest that I_{Ca} is critically required for the generation of bursting in developing CA1 pyramidal cells. However, they do not indicate which of all Ca^{2+} channel types are involved in this process.

Effects of type-selective Ca^{2+} channel blockers

Like most neurones in the CNS, CA1 pyramidal cells express multiple types of voltage-gated Ca^{2+} channels,

which may contribute differentially to bursting (Magee & Carruth, 1999; Golding *et al.* 1999; Su *et al.* 2002). In order to determine which Ca^{2+} channel types are responsible for intrinsic bursting in developing CA1 pyramidal cells, we first examined the effects of 0.1 mM Ni^{2+}, 10 μM nimodipine and 5 μM CTX, added separately or in different combinations to the ACSF. The results are illustrated in Fig. 4. Application of 0.1 mM Ni^{2+} in the ACSF consistently and reversibly suppressed bursting. In 79% (11 of 14) of the neurones, bursting was totally blocked (Fig. 4*A*), while in the other three neurones N_S decreased (Fig. 4*B*). On average, 0.1 mM Ni^{2+} decreased N_S from 2.5 ± 0.6 to 1.2 ± 0.4 ($n = 14$; $P < 0.05$), while reducing ADP duration from 32.0 ± 5.5 to 18.1 ± 6.4 ms ($n = 14$; $P < 0.05$). In cases that where only partially suppressed by 0.1 mM Ni^{2+}, subsequent addition of nimodipine totally abolished bursting and further reduced the spike ADP from 23.8 ± 7.9 to 10.7 ± 2.9 ($n = 3$; $P < 0.05$; Fig. 4*B*). Nimodipine added alone to the ACSF also suppressed bursting completely in 50% (4 of 8; Fig. 4*C*) of the neurones. In the other 50% of the neurones bursting was partially attenuated.

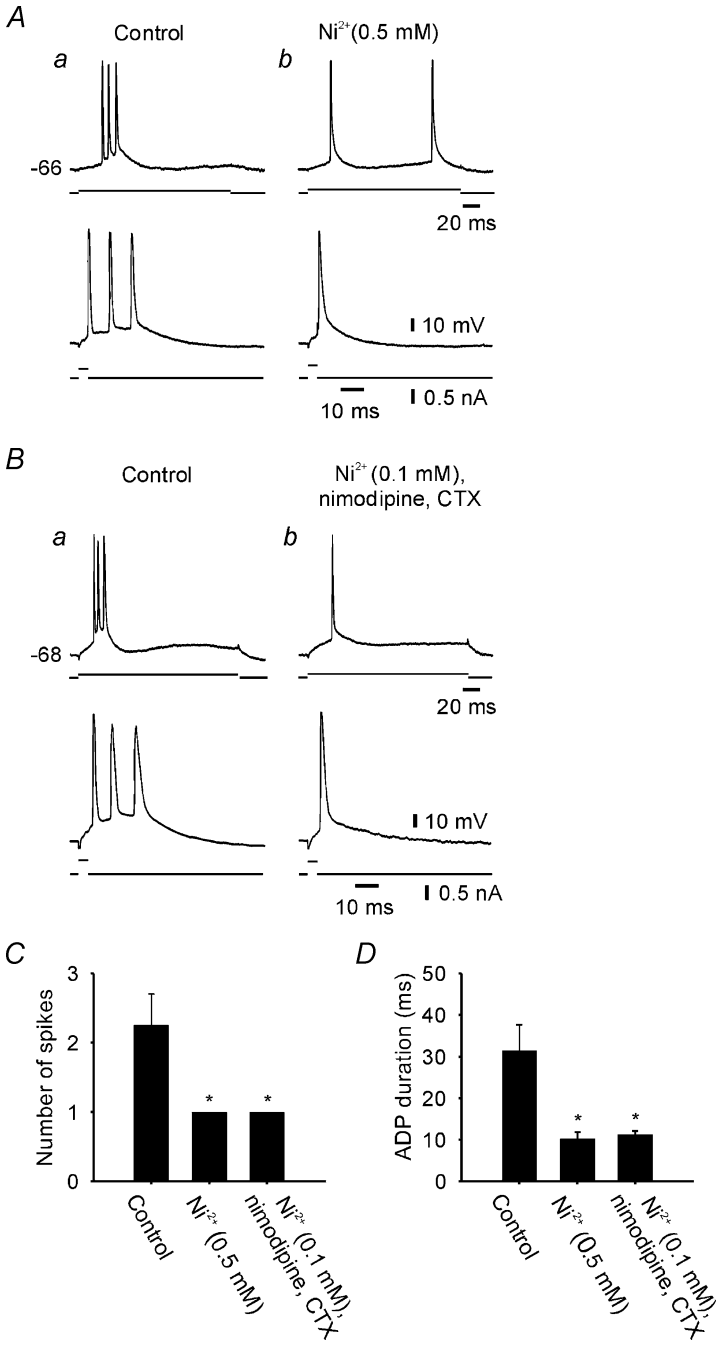

Figure 3. Blockage of voltage-gated Ca^{2+} channels abolishes intrinsic bursting in developing CA1 pyramidal cells

A, effects of 0.5 mM Ni^{+} added to the ACSF on a bursting neurone (P16). Bursting (*a*) was entirely suppressed after 15 min of exposure to Ni^{2+} (*b*). *B*, effects of ACSF containing a mixture of Ca^{2+} channel blockers on a P20 burster. The mixture comprised 0.1 mM Ni^{2+}, 10 μM nimodipine and 5 μM CTX. Bursting (*a*) was entirely suppressed after 18 min of exposure to the drugs (*b*). *C* and *D*, bar diagrams summarizing the effects of blocking voltage-gated Ca^{2+} channels on bursting (*C*) and on ADP duration (*D*) in P15–P20 neurones. *Significant compared to control ($P < 0.05$). ACSF, artificial cerebrospinal fluid; CTX, ω-conotoxin MVIIC.

On average, nimodipine decreased N_S from 2.2 ± 0.4 to 1.3 ± 0.3 ($n = 8$; $P < 0.05$), while reducing ADP duration from 32.5 ± 4.9 to 16.7 ± 7.1 ms ($n = 8$; $P < 0.05$). Subsequent addition of 0.1 mM Ni^{2+} totally abolished nimodipine-insensitive bursting and further reduced ADP duration from 21.3 ± 6.1 to 9.5 ± 1.7 ms ($n = 4$; $P < 0.05$). In contrast, exposure to CTX for up to 45 min ($n = 5$) had no effect on bursting (2.6 ± 0.5 in both control and drug groups) or on spike ADP duration (33.5 ± 9.1 and 31.6 ± 10.5 ms before and after application of CTX, respectively; Fig. 4*Da* and *b*, top traces). At the same time, however, CTX markedly reduced the orthodromically evoked excitatory postsynaptic potentials (EPSPs), confirming that the toxin reached the neurones and blocked presynaptic Ca^{2+} channels (Fig. 4*Da* and *b*, bottom traces). Addition of 10 μM nimodipine and 0.1 mM Ni^{2+} to the CTX-containing ACSF abolished both bursting and the remaining EPSP component (Fig. 4*Dc*).

The results of these experiments are summarized in Fig. 4*E* and *F*. The sensitivity of intrinsic bursting to low Ni^{2+} concentrations and to nimodipine implicates both T/R- and L-types of Ca^{2+} channels in the generation of this activity.

Focal applications of Ca^{2+} channel blockers

The densities of different types of voltage-gated Ca^{2+} channels expressed in the somatic and dendritic compartments of CNS neurones appear to change during the course of postnatal development. In CA1 pyramidal cells, for example, Ni^{2+}-sensitive T-type Ca^{2+} channels largely disappear from the somatic region during the first 2 postnatal weeks, but retain their activity in the apical dendrites (Thompson & Wong, 1991; Karst *et al.* 1993). It was therefore interesting to determine the cellular localization of the Ca^{2+} channels that generate intrinsic bursting in these neurones during the transitional period. To that end, we used a pressure ejection system connected to an application pipette (containing 5 mM Ni^{2+}) to puff Ni^{2+} focally onto the somatic region or onto the distal apical dendrites of these neurones (Fig. 1*A*; see Methods). When Ni^{2+} was puffed to the somatic region it exerted no effect on the burst response ($n = 6$; Fig. 5*Aa* and *b*, top and middle traces). The duration of the spike ADP also was unaffected by these puffs (34.5 ± 5.7 and 34.2 ± 4.6 ms before and after application of Ni^{2+}, respectively). To ensure that an effective concentration of Ni^{2+} had reached

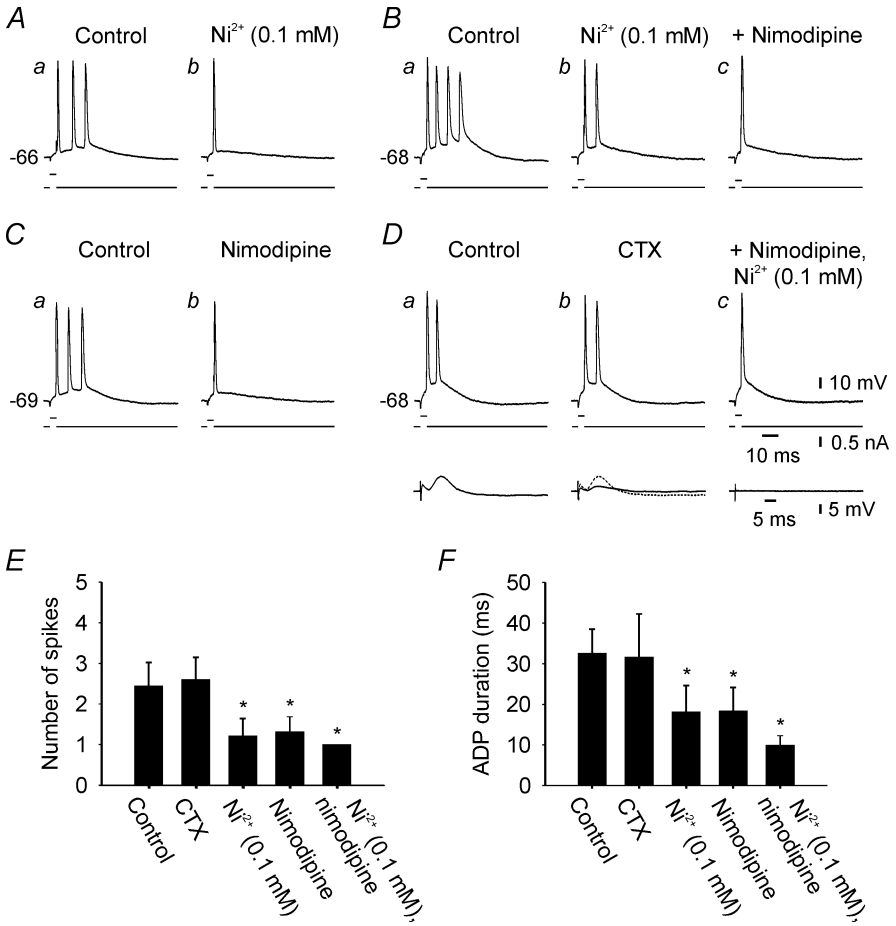

Figure 4. Contribution of different types of voltage-gated Ca^{2+} channels to bursting in developing neurones
All drugs were applied in the ACSF for at least 30 min. *A*, bursting in a P18 neurone (*a*) was fully blocked by 100 μM Ni^{2+} (*b*). *B*, bursting in a P19 neurone (*a*) was only partially blocked by 100 μM Ni^{2+} (*b*), but addition of 10 μM nimodipine blocked it completely (*c*). *C*, bursting in a P18 neurone (*a*) was fully blocked by 10 μM nimodipine (*b*). *D*, bursting in a P17 neurone (*a*, upper trace) was unaffected by 45-min exposure to 5 μM CTX (*b*, upper trace). Subsequent addition of 100 μM Ni^{2+} and 10 μM nimodipine suppressed bursting (c, upper trace). In the same neurone, CTX markedly reduced the orthodromically evoked EPSP response (*a* and *b*, bottom traces; each trace is an average of five consecutive EPSPs), indicating that presynaptic N- and P/Q-type Ca^{2+} channels were blocked. Subsequent addition of Ni^{2+} and nimodipine abolished the EPSP entirely (*c*, bottom trace). *E* and *F*, bar diagram summarizing the effects of different type-selective blockers of voltage-gated Ca^{2+} channels on bursting (*E*) and on ADP duration (*F*) in P15–P20 neurones. *Significant compared to control ($P < 0.05$). ACSF, artificial cerebrospinal fluid; CTX, ω-conotoxin MVIIC; EPSP, excitatory postsynaptic potential.

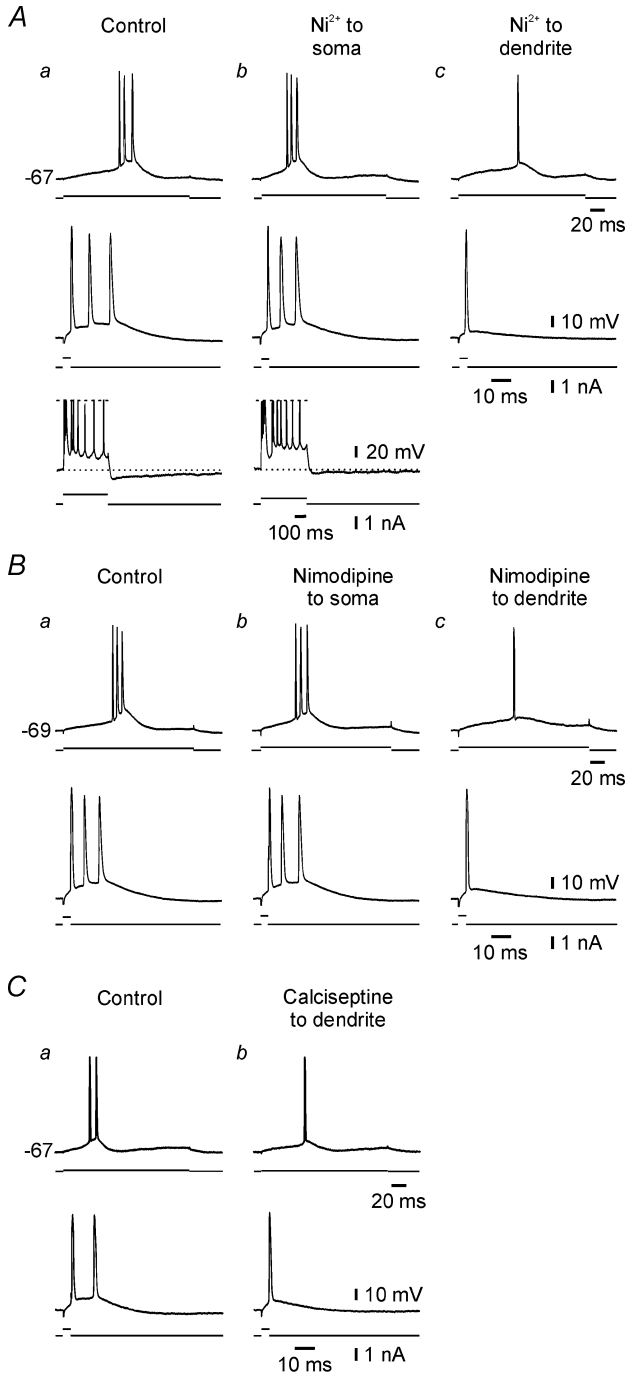

Figure 5. Blockage of Ca^{2+} channels in distal apical dendrites, but not in the somatic region, suppresses bursting in developing neurones

A, effects of focally puffed Ni^{+}. In a P18 burster (*a*), puffing Ni^{2+} onto the somatic region had no detectible effects on bursting behaviour (*b*, top and middle traces) but substantially reduced the sAHP (*b*, bottom trace; the intensity of the prolonged pulse used to evoke repetitive discharge was adjusted to trigger the same number of spikes in each condition). In contrast, Ni^{2+} puffed onto the distal apical dendrites suppressed bursting entirely. *B*, effects of focally applied nimodipine. In another P19 burster (*a*), nimodipine had no detectible effects on bursting behaviour when puffed onto the somatic region (*b*), but totally suppressed it when applied to the apical dendrites (*c*). *C*, effects of focally applied calciseptine. In another P19 burster (*a*), calciseptine totally suppressed bursting behaviour when applied to the apical dendrites (*b*). sAHP, slow afterhyperpolarization.

the soma of the impaled neurones, we also monitored the sAHP that is generated at the soma following a train of spikes (Madison & Nicoll, 1984; Bowden *et al.* 2001). Puffing Ni^{2+} onto the somatic region consistently reduced the sAHP (Fig. 5*Aa* and *b*, bottom traces), implying that somatic Ca^{2+} channels were blocked by Ni^{2+}. In contrast, when Ni^{2+} was puffed onto the distal apical dendrites at a distance of 300 μm from the soma, bursting was consistently abolished and spike ADP duration decreased from 34.2 ± 4.6 to 17.8 ± 6.1 ms ($n = 6$; $P < 0.05$; Fig. 5*Ac*, top and middle traces). A similar suppression of bursting was seen also when Ni^{2+} was puffed onto the distal apical dendrites without prior application to the somatic region ($n = 4$; data not shown).

Analogous experiments were performed with nimodipine (100 μM in the puffing pipette). In five such experiments, nimodipine had no detectible effects on N_s (from 2.2 ± 0.9 to 2.5 ± 0.5) and spike ADP duration (from 27.2 ± 11.0 to 29.7 ± 10.5 ms) when applied to the somatic region (Fig. 5*Ba* and *b*). However, when puffed onto the distal apical dendrites, nimodipine partially suppressed bursting (from 2.5 ± 0.5 to 1.2 ± 0.2 spikes; $P < 0.05$) and significantly reduced the spike ADP duration (from 29.7 ± 10.5 to 21.3 ± 9.2 ms; $P < 0.05$; Fig. 5*Bc*).

Several studies have indicated that in addition to blocking L-type Ca^{2+} channels, some dihydropyridine compounds may also block T-type Ca^{2+} channels (Takahashi & Akaike, 1991; Stengel *et al.* 1998; but see Avery & Johnston, 1996). Therefore, we cannot exclude the possibility that the effects of nimodipine described here are mediated at least in part by T-type Ca^{2+} channel block. We sought to obtain additional evidence concerning the involvement of L-type Ca^{2+} channels in bursting by testing the effects of calciseptine. This snake neurotoxin was shown to block only L-type Ca^{2+} channels (De Weille *et al.* 1991). When puffed onto the apical dendrites (from an application pipette containing 10 μM), calciseptine suppressed bursting in 5 out of 6 neurones (Fig. 5*C*). It significantly reduced N_S (from 2.0 ± 0.0 to 1.2 ± 0.4 spikes; $P < 0.05$), as well as the spike ADP duration (from 27.8 ± 6.6 to 18.0 ± 4.2 ms; $P < 0.05$).

Cumulatively, these data strongly suggest that the T/R- and L-type Ca^{2+} channels that are responsible for intrinsic bursting, reside predominantly in the distal apical dendrites of developing CA1 pyramidal cells.

Effects of the L-type channel agonist BAY-K8644

Given the supportive role of L-type Ca^{2+} channels in bursting behaviour in developing CA1 pyramidal

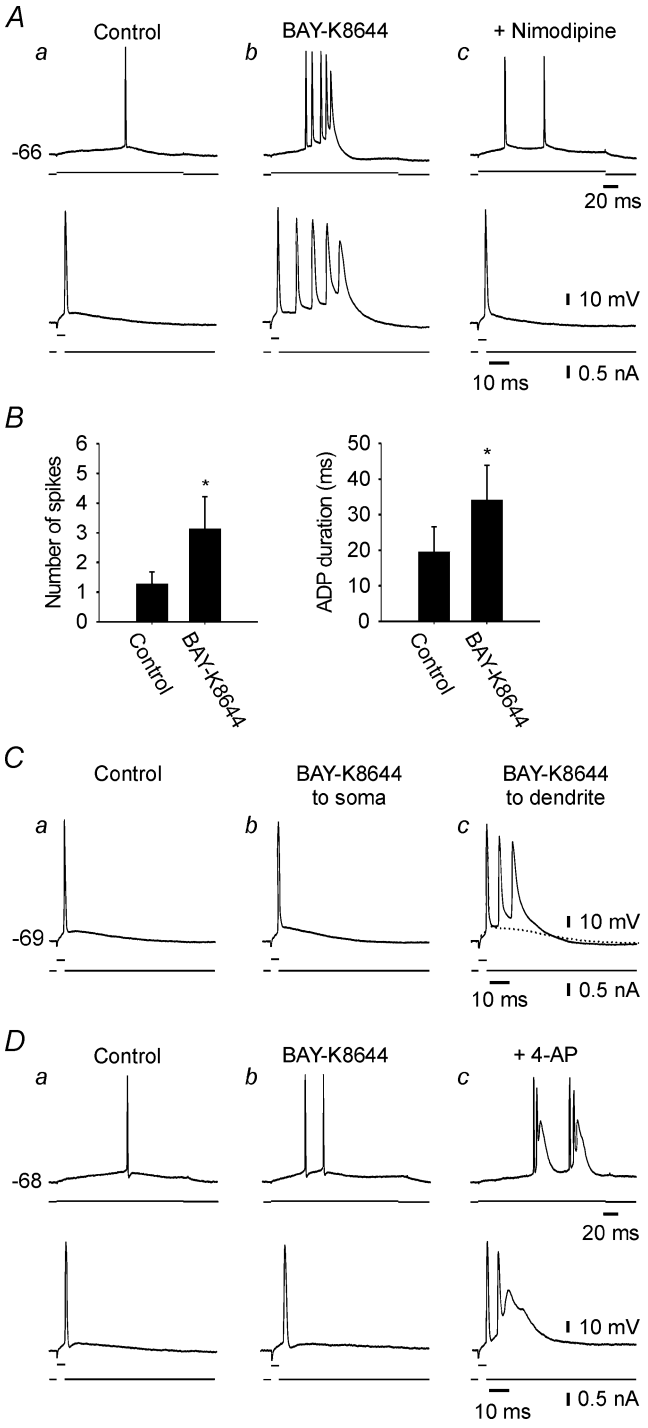

Figure 6. Augmentation of L-type I_{Ca} in distal apical dendrites can induce bursting in developing neurones
A, in a P19 non-burster (*a*), adding 1 μM BAY-K8644 to the ACSF induced bursting behaviour within 13 min (*b*), which was suppressed by subsequent addition of 10 μM nimodipine (*c*). *B*, bar diagram summarizing the effects of BAY-K8644 on bursting behaviour (left) and on ADP duration (right) in P16-P20 neurones. *Significant compared to control ($P < 0.05$). *C*, effects of focally applied BAY-K8644. In another P17 non-burster (*a*), BAY-K86644 slightly enhanced the spike ADP when puffed onto the somatic region (*b*). When applied to the distal apical dendrites, it caused a progressive facilitation of the spike ADP (*c*, dotted trace) until it was sufficiently large to trigger a burst (*c*, solid trace). *D*, in an adult neurone (*a*), adding 1 μM BAY-K8644 to the ACSF for 30 min had no effect on discharge behaviour (*b*). Subsequently adding 3 mM 4-AP to the ACSF induced bursting within 10 min which was suppressed by subsequent addition of 10 μM nimodipine (*c*). ACSF, artificial cerebrospinal fluid; 4-AP, 4-aminopyridine; ADP, afterdepolarization.

cells, we wondered whether increasing L-type I_{Ca} would augment bursting or induce it in non-bursters. We increased this current by adding 1 μM BAY-K8644 to the ACSF (Fox *et al.* 1987; McCarthy & TanPiengco, 1992; Magee & Johnston, 1995). In six non-bursters and two bursters (P15–P20), exposure to this L-type channel agonist progressively prolonged the spike ADP (from 19.5 ± 7.0 to 34.1 ± 9.6 ms; $P < 0.05$) and enhanced or induced bursting in all cases (N_S increased from 1.2 ± 0.3 to 3.1 ± 1.0; $P < 0.05$). This effect is illustrated in Fig. 6*Aa* and *b*. The changes induced by BAY-K8644 were reversed by adding 10 μM nimodipine to the ACSF (Fig. 6*Ac*). Figure 6*B* summarizes the main findings of these experiments.

In another series of experiments we focally puffed BAY-K8644 (10 μM in the pipette) onto the somatic region or onto the distal apical dendrites of five non-bursters (P15–P20). Somatic applications of this drug had no consistent effects on the duration of the spike ADP in these neurones (23.9 ± 7.5 ms in control *versus* 21.5 ± 13.5 ms in the presence of BAY-K8644; Fig. 6*Ca* and *b*). In one of these neurones, however, somatic puffing of BAY-K8644 prolonged the ADP and induced a second spike (data not shown; therefore the average N_S evoked by brief stimuli increased from 1.0 ± 0.0 to 1.2 ± 0.4). In contrast, distal dendritic puffing of BAY-K8644 consistently induced or enhanced bursting in all five neurones (from 1.2 ± 0.4 to 3.4 ± 1.5 spikes; $P < 0.05$; Fig. 6*Cc*) and markedly prolonged the spike ADP (from 21.5 ± 13.5 to 45.3 ± 11.6 ms; $P < 0.05$). These data further support the notion that L-type Ca^{2+} channels involved in bursting are contained primarily in the distal apical dendrites of developing CA1 pyramidal cells.

For comparison, we examined the effects of BAY-K8644 in six adult (> P30) CA1 pyramidal cells. A representative experiment is shown in Fig. 6*D*. In all these neurones, the response to threshold-straddling stimuli was a single spike (Fig. 6*Da*). Adding 1 μM BAY-K8644 had no effect on discharge behaviour in all cases (Fig. 6*Db*). Likewise, spike ADP duration did not change significantly in the presence of BAY-K8644 (from 22.2 ± 9.4 to 18.9 ± 5.9 ms; $n = 6$). However, adding 3 mM 4-AP to the ACSF consistently induced bursting in these neurones (Fig. 6*Dc*).

Application of tetrodotoxin to the apical dendrites

Activation of Ca^{2+} channels in the distal apical dendrites following a somatically generated spike would require

spike backpropagation into these dendrites (Jaffe *et al.* 1992; Spruston *et al.* 1995). Thus, intrinsic bursting in developing CA1 pyramidal cells may critically depend on the backpropagation of the somatic spike. If that is the case, then bursting should be blocked by application of TTX to the apical dendrites (Magee & Carruth, 1999). We tested this notion by puffing TTX (0.1 μM in the application pipette) onto the distal apical dendrites (at a distance of 300 μm from the soma) in five bursters. In all these experiments and as illustrated in Fig. 7, TTX totally suppressed the burst responses and markedly reduced the ADP duration (from 29.2 ± 6.3 to 12.0 ± 1.6 ms; $P < 0.05$; Fig. 7*A* and *B*). The threshold, rise time and amplitude of the first spike were not concurrently affected by distally puffed TTX (Fig. 7*C*), indicating that its action was confined to the apical dendrites. As expected, when TTX was puffed onto the somatic region, it quickly suppressed all spike activity (data not shown).

Effects of the I_{NaP} blocker riluzole

The above findings are consistent with the hypothesis that bursting in developing CA1 pyramidal cells results from somatic spike backpropagation into the distal apical dendrites, where it activates distinct types of Ca^{2+} channels that generate a local Ca^{2+} spike. This, in turn, spreads to the soma where it augments the somatic spike ADP, thereby inducing multiple firing. But is this sequence of events sufficient to produce bursting? Recent studies in adult CA1 pyramidal cells have shown that I_{NaP} may also contribute to intrinsic bursting in some conditions (Jensen *et al.* 1996; Su *et al.* 2001). In cortical neurones, low concentrations of riluzole reduce I_{NaP} without markedly affecting the transient Na^+ current (Urbani & Belluzzi, 2000). Therefore, to evaluate the role of I_{NaP} in bursting behaviour of developing CA1 pyramidal cells, we examined its modulation by riluzole.

In four bursting neurones (P17–P19), adding 10 μM riluzole to the ACSF for 30 min did not significantly alter resting membrane potential (from -70.4 ± 2.5 to -71.3 ± 3.5 mV; $n = 4$) or input resistance (from 39.7 ± 7.9 to 50.9 ± 12.6 MΩ; $n = 4$). As illustrated in Fig. 8*A*, 10 μM riluzole consistently abolished bursting (from 2.3 ± 0.5 to 1.0 ± 0.0 spikes; $P < 0.05$), while

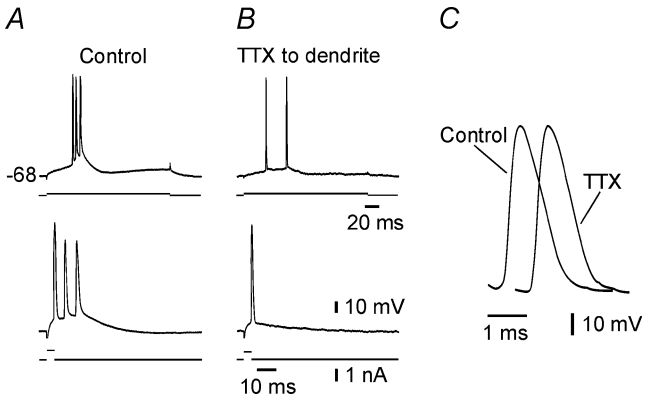

Figure 7. Application of TTX to apical dendrites suppresses bursting in apical neurones
In a P18 burster (*A*), puffing TTX onto the apical dendrites suppressed bursting entirely within 4 min, without affecting spike threshold (*B*). The first spikes evoked by brief pulses (*A* and *B*, bottom traces) are overlaid in *C*. The rise times and amplitudes of these spikes were also unaffected by dendritic TTX application.

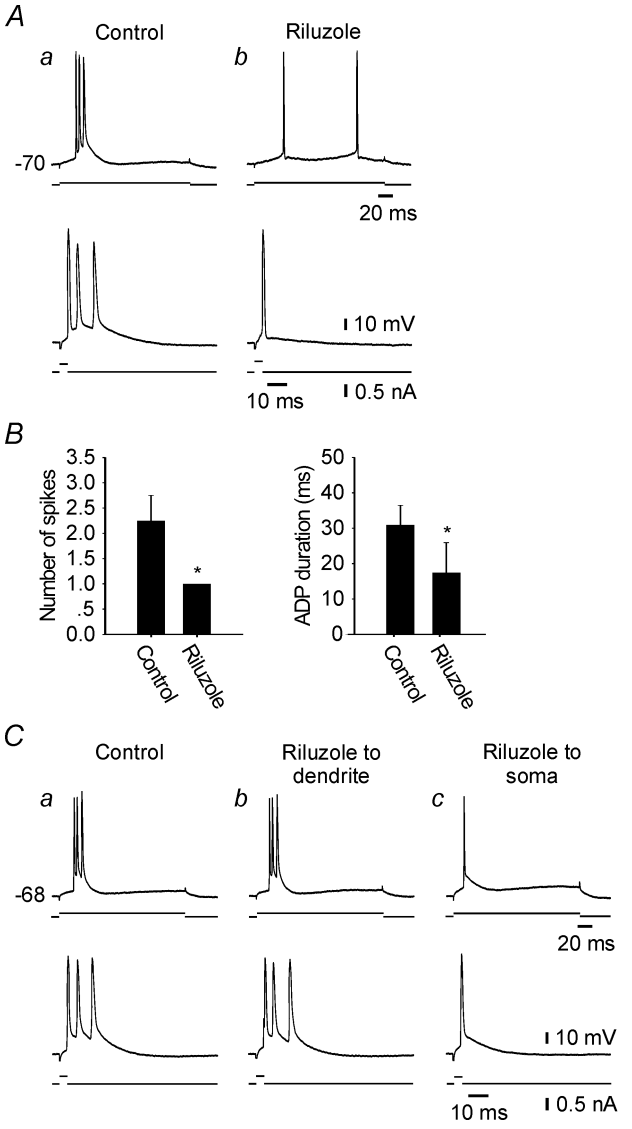

Figure 8. Inhibition of persistent Na^+ channels in the somatic region suppresses bursting in developing neurones
A, in a P18 burster (*a*), adding 10 μM riluzole to the ACSF suppressed bursting behaviour within 23 min (*b*). *B*, bar diagram summarizing the effects of riluzole on bursting behaviour (left) and on ADP duration (right) in P16–P19 neurones. *Significant compared to control ($P < 0.05$). *C*, effects of focally applied riluzole. In another P17 burster (*a*), riluzole had no detectible effect when puffed onto the distal apical dendrites (*b*). When puffed onto the somatic region it abolished bursting within 9 min (*c*). ACSF, artificial cerebrospinal fluid.

markedly reducing the spike ADP duration (from 30.8 ± 5.6 to 17.3 ± 8.5 ms; $P < 0.05$). These effects are summarized in Fig. 8*B*.

Because riluzole was shown also to open small-conductance Ca^{2+}-activated K^+ channels in hippocampal neurones (Cao *et al.* 2002), we repeated these experiments with ACSF containing 50 nM apamin, a potent blocker of these channels in CA1 pyramidal cells (Stocker *et al.* 1999). Apamin itself had no effect on bursting in developing neurones, whereas 10 μM riluzole consistently blocked this activity in its presence ($n = 4$; data not shown).

We further sought to identify the cellular localization of riluzole's action. Therefore, we puffed riluzole (100 μM in the pipette) onto the distal apical dendrites or the somatic region of four CA1 pyramidal cells. When puffed onto the distal apical dendrites, riluzole affected neither N_S (2.3 ± 0.5 spikes in control and in the presence of riluzole) nor spike ADP duration (from 28.9 ± 2.8 to 26.6 ± 3.17 ms; Fig. 8*Ca* and *b*). In contrast, when puffed onto the somatic region, riluzole totally suppressed bursting and significantly reduced the duration of the spike ADPs (from 26.6 ± 3.17 to 13.5 ± 2.0 ms; $P < 0.05$; $n = 4$; Fig. 8*Cc*).

Our finding that riluzole blocks bursting only when applied to the proximal region of the neurone excludes the possibility that it acts by blocking voltage-gated Ca^{2+} channels (Stefani *et al.* 1997) or glutamate release (Prakriya & Mennerick, 2000). Such effects, if present in CA1 pyramidal cells, should be evident upon focal application of riluzole to the apical dendrites. The most parsimonious explanation for our data is that activation of persistent Na^+ channels at or near the soma is also a prerequisite for burst generation in developing CA1 pyramidal cells.

Impact of intrinsic bursting on synaptically evoked discharge

Neurones that fire bursts in response to brief depolarizing current pulses would be expected to do so also when activated by an EPSP. In reality, however, synaptic excitation of CA1 pyramidal cells is confounded by feedforward and feedback inhibition, which may curtail the evoked burst (Turner, 1990). To explore whether intrinsic bursting in developing neurones can be recruited synaptically, we compared the spike discharge evoked by threshold-straddling EPSPs in bursting *versus* non-bursting firing P15–P20 neurones. Single-shock stimuli were applied in stratum radiatum near the CA2–CA3 border at 0.2 Hz. Stimulation intensity was adjusted to obtain threshold-straddling EPSPs. These EPSPs evoked a single spike in all non-bursters examined ($n = 6$; Fig. 9*A*), as well as in 50% (5/10) of bursting neurones (Fig. 9*B*). In the other 50% of bursters, the synaptically evoked discharge comprised the same number of spikes as in the intrinsic burst (Fig. 9*C*). Thus, on average, bursting neurones fire more spikes than non-bursters in response to similar EPSPs. The cases in which synaptic burst recruitment fail most probably are due to concurrently activated postsynaptic inhibition.

Discussion

In this study we have identified a transitional period between P12 and P25 in which CA1 pyramidal cells first acquire, and than lose, the propensity to generate high-frequency bursts of two or more spikes as their minimal suprathreshold response. In the middle of this period, 74% of CA1 pyramidal cells display a bursting phenotype, compared to 3% before, and 6% after, this period. Given that bursting neurones have a unique impact on neuronal plasticity and integration (Kepecs & Lisman, 2003), such an increase in the fraction of bursters must have dramatic consequences for hippocampal development and maturation.

A tendency of developing CA1 pyramidal cells to fire spike doublets has been noted previously (Costa *et al.* 1991). Here we expand this initial observation and investigate its ionic mechanism. Our findings suggest that intrinsic bursting in developing neurones results from 'ping-pong' interplay between spike afterpotentials in soma and in distal apical dendrites, similar to that found in 4-AP-treated adult CA1 pyramidal cells (Magee & Carruth, 1999). According to this model, a spike initiated at the proximal axon back-propagates into the soma and apical

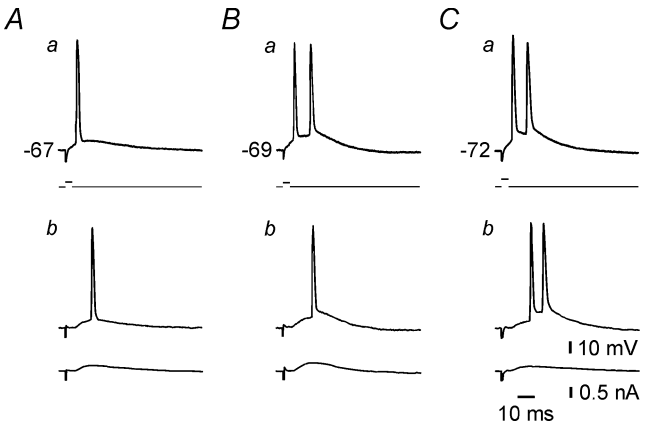

Figure 9. Intrinsic bursts can be recruited synaptically
A, in a P19 non-burster (*a*), orthodromic stimulation at 0.2 Hz was adjusted to evoke threshold-straddling EPSPs that sometimes did (*b*, top trace), and sometimes did not, evoke spike discharge (*b*, bottom trace). The EPSPs that reached threshold induced one spike only (*b*, top trace). *B*, in a P15 burster (*a*), similar EPSPs also evoked a single spike (*b*) despite the double spike responses to brief depolarizing current pulses (*a*). *C*, in a P16 burster (*a*), threshold-straddling EPSPs were either subthreshold (*b*, bottom trace), or triggered a double spike response (*b*, top trace), similar to that evoked by brief depolarizing current pulses (*a*).

dendrites (Spruston *et al.* 1995; Colbert & Johnston, 1996). The extent of dendritic invasion and depolarization by this spike depends on the density ratio of inward (Na^+ and Ca^{2+}) to outward (K^+) currents that co-activate during this process (Johnston *et al.* 1999). In adult CA1 pyramidal cells this ratio is low, so that a back-propagating spike is attenuated in the proximal dendrite and its impact on the somatic spike ADP is small (Hoffman *et al.* 1997). In this case the ADP is derived predominantly from activation of proximal I_{NaP} and is too small to initiate a regenerative burst response (Azouz *et al.* 1996; Su *et al.* 2001). However, if the inward to outward current density ratio is high, as may be the case in developing neurones between P12 and P25, the back-propagating spike would be much less attenuated and may trigger a dendritic Ca^{2+} spike. The latter spike, in turn, spreads proximally and augments the I_{NaP}-driven spike ADP at the somatic region, leading to the generation of a spike burst.

Our results support this proposed scheme. Firstly, bursting is suppressed by TTX application to the apical dendrites, indicating a requirement for spike back-propagation. This effect of TTX cannot be due to inhibition of dendritic I_{NaP}, because riluzole, which blocks this current, has no effect on bursting when applied at the same location. Secondly, bursting is suppressed by application of Ni^{2+} or nimodipine to the distal apical dendrites, but not to the somatic region, demonstrating that dendritic Ca^{2+} electrogenesis is crucial for this process. Thirdly, bursting is suppressed by riluzole application to the somatic region, indicating that activation of I_{NaP} at or near the soma also is essential for the evolution of a spike burst.

In adult CA1 pyramidal cells, back-propagating spikes activate Ca^{2+} channels in the apical dendrites (Jaffe *et al.* 1992; Spruston *et al.* 1995), but do not ordinarily evoke regenerative Ca^{2+} spikes. Presumably such an escalation is prevented by co-activation of fast inactivating K^+ channels (A-type), whose density along the apical dendrite increases with distance from the soma (Hoffman *et al.* 1997). Blocking these channels with millimolar 4-AP facilitates spike invasion into dendritic branches and allows the development of a dendritic Ca^{2+} spike that, in turn, triggers somatic bursting. The dendritic Ca^{2+} channels involved in this activity also are predominantly of the T/R- and L-type (Magee & Carruth, 1999). Here we show that natural bursting in developing neurones is generated by the same types of Ca^{2+} channels. These findings are consistent with the predominant expression of T/R-type Ca^{2+} channels in distal apical dendrites of CA1 pyramidal cells (Christie *et al.* 1995; Magee & Johnston, 1997; Kavalali *et al.* 1997). Though we could not differentiate pharmacologically between T- and R-type channels, it is more likely that T-type channels underlie bursting, given their much lower threshold of activation and slower deactivation kinetics (Randall & Tsien, 1997; Su *et al.* 2002). It is less clear why L-type Ca^{2+} channels in distal apical dendrites are critical for bursting, as these channels reportedly aggregate mostly in the soma and proximal dendrites (Hell *et al.* 1993; Magee & Johnston, 1995; Christie *et al.* 1995).

A high ratio of inward to outward current density in developing neurones may be due to over-expression of Ca^{2+} and Na^+ channels and/or under-expression of K^+ channels compared to adult values. In CA1 pyramidal cells, the density of Ca^{2+} channels increase after birth and reaches adult values at P13 and P20, respectively (Kortekaas & Wadman, 1997). These changes, as well as the presumed translocation of T-type Ca^{2+} channels from soma to apical dendrites (Thompson & Wong, 1991; Karst *et al.* 1993), may underlie the appearance of intrinsic bursting between P12 and P18. A developmental increase in the density of I_{NaP} may also contribute to the appearance of intrinsic bursting, as this current also appears essential for this behaviour. On the other hand, the disappearance of bursting between P18 and P25 may be due to a late increase in density of functional A-type K^+ channels in apical dendrites, which would counteract the depolarizing actions of I_{Ca}. Indeed, blocking these channels with millimolar 4-AP induced Ca^{2+}-dependent bursting in 18 of 20 adult CA1 pyramidal cells (C. Yue, S. Chen and Y. Yaari, unpublished observations). Our finding that BAY-K8644 induces Ca^{2+}-dependent bursting that originates in apical dendrites in developing, but not in adult CA1 pyramidal cells, also suggests that the latter neurones are less prone to dendritic Ca^{2+} electrogenesis than their young counterparts.

In adult neocortical pyramidal cells, backpropagating spikes were shown to trigger a dendritic Ca^{2+} spike and somatic bursting, provided spike invasion of the apical dendrites coincided with a distal dendritic EPSP (Larkum *et al.* 1999). Presumably the depolarization of the apical dendrites either by a single backpropagating spike or by an EPSP, is insufficient to set off a local Ca^{2+} spike. However, when the two potentials coincide, the total depolarization of the dendrites is adequately large to elicit a local Ca^{2+} spike, which in turn triggers somatic bursting.

Neonatal CA1 pyramidal cells display spontaneous *network* bursting that is driven by depolarizing GABAergic postsynaptic potentials. This activity disappears by P15–P16 with the maturation of GABAergic inhibition (Ben-Ari, 2002). During network-driven bursts individual neurones generate a synaptically driven burst of high-frequency (up to 100 Hz) spikes associated with a large increase in intracellular Ca^{2+} concentration (Garaschuk *et al.* 1998). The marked increase in *intrinsic* bursting described in this report temporally parallels the disappearance of early network bursting and attains maximum expression a few days after network bursting fades out. It is interesting that this sequence of developmental events can be recapitulated in the adult brain by inducing intense network bursting (i.e. seizure

activity) with the convulsant pilocarpine. A few days after such treatment, intrinsic bursting appears in over 50% of regular-firing CA1 pyramidal cells (Sanabria *et al.* 2001). Like the natural intrinsic bursts in developing neurones, intrinsic bursts induced by seizure activity in adult neurones also are Ni^{2+} sensitive (Su *et al.* 2002), and also require Ca^{2+} electrogenesis in the apical dendrites (C. Yue, H. Su and Y. Yaari, unpublished observations). The hypothesis that early network bursting triggers the molecular changes underlying the subsequent appearance of intrinsic bursting is based on these similarities.

It has been hypothesized that early network bursting is germane to the establishment of synaptic connectivity during postnatal development. Presumably the early population bursts furnish the necessary pre- and post-synaptic coincident activity for transforming silent synapses into active ones (Durand *et al.* 1996) and for strengthening weakly connected synapses (Kasyanov *et al.* 2004). It is therefore tempting to speculate that the appearance of intrinsic bursting in CA1 pyramidal cells serves a further important role in modifying synaptic connectivity. Indeed, the transitional period of intrinsic bursting is also a period of intense proliferation and ramification of apical dendrites and formation of excitatory synapses on dendritic spines in these neurones (Pokorny & Yamamoto, 1981*a*,*b*). Likewise, the ability of CA1 pyramidal cells to undergo long-term potentiation in response to high-frequency (100 Hz) stimulation of afferent fibres becomes consistent only after P12 (Harris & Teyler, 1984; Muller *et al.* 1989), which is about the time of first appearance of bursting pyramidal cells (Fig. 2*B*). What can be the role of intrinsic bursting in these processes? Many studies have shown that both activity-dependent synaptogenesis and long-term potentiation of synaptic strength require activation of postsynaptic *N*-methyl-D-aspartate (NMDA) receptors and an increase in intradendritic Ca^{2+} levels (Muller *et al.* 2002). Clearly, a postsynaptic spike burst driven by a dendritic Ca^{2+} spike would be extremely effective in unblocking of postsynaptic NMDA receptor channels by Mg^{2+} and in raising dendritic Ca^{2+} levels in comparison with a solitary back-propagating spike that only partially invades the apical dendrites (Magee & Johnston, 1997). Consequently, the transitional period of intrinsic bursting during postnatal development may also be a period of heightened NMDA receptor-dependent synaptic plasticity.

References

Avery RB & Johnston D (1996). Multiple channel types contribute to the low-voltage-activated calcium current in hippocampal CA3 pyramidal neurons. *J Neurosci* **16**, 5567–5582.

Azouz R, Jensen MS & Yaari Y (1996). Ionic basis of spike after-depolarization and burst generation in adult rat hippocampal CA1 pyramidal cells. *J Physiol* **492**, 211–223.

Ben-Ari Y (2002). Excitatory actions of GABA during development: the nature of the nurture. *Nat Rev Neurosci* **3**, 728–739.

Bowden SE, Fletcher S, Loane DJ & Marrion NV (2001). Somatic colocalization of rat SK1 and D class (Ca_v 1.2), L–type calcium channels in rat CA1 hippocampal pyramidal neurons. *J Neurosci* **21**, RC175 1–6.

Cao YJ, Dreixler JC, Couey JJ & Houamed KM (2002). Modulation of recombinant and native neuronal SK channels by the neuroprotective drug riluzole. *Eur J Pharmacol* **449**, 47–54.

Catterall WA (2000). Structure and regulation of voltage-gated Ca^{2+} channels. *Ann Rev cell Dev Biol* **16**, 521–555.

Christie BR, Eliot LS, Ito K, Miyakawa H & Johnston D (1995). Different Ca^{2+} channels in soma and dendrites of hippocampal pyramidal neurons mediate spike-induced Ca^{2+} influx. *J Neurophysiol* **73**, 2553–2557.

Colbert CM & Johnston D (1996). Axonal action-potential initiation and Na^+ channel densities in the soma and axon initial segment of subicular pyramidal neurons. *J Neurosci* **16**, 6676–6686.

Costa PF, Ribeiro MA & Santos AI (1991). Afterpotential characteristics and firing patterns in maturing rat hippocampal CA1 neurones in in vitro slices. *Brain Res Dev Brain Res* **62**, 263–272.

De Weille JR, Schweitz H, Maes P, Tartar A & Lazdunski M (1991). Calciseptine, a peptide isolated from black mamba venom, is a specific blocker of the L-type calcium channel. *Proc Natl Acad Sci U S A* **88**, 2437–2440.

Durand GM, Kovalchuk Y & Konnerth A (1996). Long-term potentiation and functional synapse induction in developing hippocampus. *Nature* **381**, 71–75.

Fox AP, Nowycky MC & Tsien RW (1987). Single-channel recordings of three types of calcium channels in chick sensory neurones. *J Physiol* **394**, 173–200.

Garaschuk O, Hanse E & Konnerth A (1998). Developmental profile and synaptic origin of early network oscillations in the CA1 region of rat neonatal hippocampus. *J Physiol* **507**, 219–236.

Golding NL, Jung HY, Mickus T & Spruston N (1999). Dendritic calcium spike initiation and repolarization are controlled by distinct potassium channel subtypes in CA1 pyramidal neurons. *J Neurosci* **19**, 8789–8798.

Harris KM & Teyler TJ (1984). Developmental onset of long-term potentiation in area CA1 of the rat hippocampus. *J Physiol* **346**, 27–48.

Hell JW, Westenbroek RE, Warner C, Ahlijanian MK, Prystay W, Gilbert MM, Snutch TP & Catterall WA (1993). Identification and differential subcellular localization of the neuronal class C and class D L-type calcium channel alpha 1 subunits. *J Cell Biol* **123**, 949–962.

Hoffman DA, Magee JC, Colbert CM & Johnston D (1997). K^+ channel regulation of signal propagation in dendrites of hippocampal pyramidal neurons. *Nature* **387**, 869–875.

Jaffe DB, Johnston D, Lasser-Ross N, Lisman JE, Miyakawa H & Ross WN (1992). The spread of Na^+ spikes determines the pattern of dendritic Ca^{2+} entry into hippocampal neurons. *Nature* **357**, 244–246.

Jensen MS, Azouz R & Yaari Y (1994). Variant firing patterns in rat hippocampal pyramidal cells modulated by extracellular potassium. *J Neurophysiol* **71**, 831–839.

Jensen MS, Azouz R & Yaari Y (1996). Spike after-depolarization and burst generation in adult rat hippocampal CA1 pyramidal cells. *J Physiol* **492**, 199–210.

Johnston D, Hoffman DA, Colbert CM & Magee JC (1999). Regulation of back-propagating action potentials in hippocampal neurons. *Curr Opin Neurobiol* **9**, 288–292.

Jung HY, Staff NP & Spruston N (2001). Action potential bursting in subicular pyramidal neurons is driven by a calcium tail current. *J Neurosci* **21**, 3312–3321.

Karst H, Jöels M & Wadman WJ (1993). Low-threshold calcium current in dendrites of the adult rat hippocampus. *Neurosci Lett* **164**, 154–158.

Kasyanov AM, Safiulina VF, Voronin LL & Cherubini E (2004). GABA-mediated giant depolarizing potentials as coincidence detectors for enhancing synaptic efficacy in the developing hippocampus. *Proc Natl Acad Sci U S A* **101**, 3967–3972.

Kavalali ET, Zhuo M, Bito H & Tsien RW (1997). Dendritic Ca^{2+} channels characterized by recordings from isolated hippocampal dendritic segments. *Neuron* **18**, 651–663.

Kepecs A & Lisman J (2003). Information encoding and computation with spikes and bursts. *Network* **14**, 103–118.

Kortekaas P & Wadman WJ (1997). Development of HVA and LVA calcium currents in pyramidal CA1 neurons in the hippocampus of the rat. *Brain Res Dev Brain Res* **101**, 139–147.

Larkum ME, Zhu JJ & Sakmann B (1999). A new cellular mechanism for coupling inputs arriving at different cortical layers. *Nature* **398**, 338–341.

McCarthy RT & TanPiengco PE (1992). Multiple types of high-threshold calcium channels in rabbit sensory neurons: high-affinity block of neuronal L-type by nimodipine. *J Neurosci* **12**, 2225–2234.

Madison DV & Nicoll RA (1984). Control of the repetitive discharge of rat CA1 pyramidal neurones *in vitro*. *J Physiol* **354**, 319–331.

Magee JC & Carruth M (1999). Dendritic voltage-gated ion channels regulate the action potential firing mode of hippocampal CA1 pyramidal neurons. *J Neurophysiol* **82**, 1895–1901.

Magee JC & Johnston D (1995). Characterization of single voltage-gated Na^+ and Ca^{2+} channels in apical dendrites of rat CA1 pyramidal neurons. *J Physiol* **487**, 67–90.

Magee JC & Johnston DA (1997). A synaptically controlled, associative signal for Hebbian plasticity in hippocampal neurons. *Science* **275**, 209–213.

Moody WJ (1998). Control of spontaneous activity during development. *J Neurobiol* **37**, 97–109.

Muller D, Nikonenko I, Jourdain P & Alberi S (2002). LTP, memory and structural plasticity. *Curr Mol Med* **2**, 605–611.

Muller D, Oliver M & Lynch G (1989). Developmental changes in synaptic properties in hippocampus of neonatal rats. *Brain Res Dev Brain Res* **49**, 105–114.

Pokorny J & Yamamoto T (1981*a*). Postnatal ontogenesis of hippocampal CA1 area in rats. I. Development of dendritic arborisation in pyramidal neurons. *Brain Res Bull* **7**, 113–120.

Pokorny J & Yamamoto T (1981*b*). Postnatal ontogenesis of hippocampal CA1 area in rats. II. Development of ultrastructure in stratum lacunosum and moleculare. *Brain Res Bull* **7**, 121–130.

Prakriya M & Mennerick S (2000). Selective depression of low-release probability excitatory synapses by sodium channel blockers. *Neuron* **26**, 671–682.

Randall AD & Tsien RW (1997). Contrasting biophysical and pharmacological properties of T-type and R-type calcium channels. *Neuropharmacology* **36**, 879–893.

Sanabria ER, Su H & Yaari Y (2001). Initiation of network bursts by Ca^{2+}-dependent intrinsic bursting in the rat pilocarpine model of temporal lobe epilepsy. *J Physiol* **532**, 205–216.

Schwartzkroin PA (1975). Characteristics of CA1 neurons recorded intracellularly in the hippocampal in vitro slice preparation. *Brain Res* **85**, 423–436.

Schwartzkroin PA & Kunkel DD (1982). Electrophysiology and morphology of the developing hippocampus of fetal rabbits. *J Neurosci* **2**, 448–462.

Spitzer NC, Kingston PA, Manning TJ & Conklin MW (2002). Outside and in: development of neuronal excitability. *Curr Opin Neurobiol* **12**, 315–323.

Spitzer NC & Ribera AB (1998). Development of electrical excitability in embryonic neurons: mechanisms and roles. *J Neurobiol* **37**, 190–197.

Spruston N, Schiller Y, Stuart G & Sakmann B (1995). Activity-dependent action potential invasion and calcium influx into hippocampal CA1 dendrites. *Science* **268**, 297–300.

Stengel W, Jainz M & Andreas K (1998). Different potencies of dihydropyridine derivatives in blocking T-type but not L-type Ca^{2+} channels in neuroblastoma-glioma hybrid cells. *Eur J Pharmacol* **342**, 339–345.

Stocker M, Kraus M & Pedarzani P (1999). An apamin-sensitive Ca^{2+}-activated K^+ current in hippocampal pyramidal neurons. *Proc Natl Acad Sci U S A* **96**, 4662–4667.

Stefani A, Spadoni F & Bernardi G (1997). Differential inhibition by riluzole, lamotrigine, and phenytoin of sodium and calcium currents in cortical neurons: implications for neuroprotective strategies. *Exp Neurol* **147**, 115–122.

Su H, Alroy G, Kirson ED & Yaari Y (2001). Extracellular calcium modulates persistent sodium current-dependent burst-firing in hippocampal pyramidal neurons. *J Neurosci* **21**, 4173–4182.

Su H, Sochivko D, Becker A, Chen J, Jiang Y, Yaari Y & Beck H (2002). Upregulation of a T-type Ca^{2+} channel causes a long-lasting modification of neuronal firing mode after status epilepticus. *J Neurosci* **22**, 3645–3655.

Takahashi K & Akaike N (1991). Calcium antagonist effects on low-threshold (T-type) calcium current in rat isolated hippocampal CA1 pyramidal neurons. *J Pharmacol Exp Ther* **256**, 169–175.

Thompson SM & Wong RK (1991). Development of calcium current subtypes in isolated rat hippocampal pyramidal cells. *J Physiol* **439**, 671–689.

Turner DA (1990). Feed-forward inhibitory potentials and excitatory interactions in guinea-pig hippocampal pyramidal cells. *J Physiol* **422**, 333–350.

Urbani A & Belluzzi O (2000). Riluzole inhibits the persistent sodium current in mammalian CNS neurons. *Eur J Neurosci* **12**, 3567–3574.

Yue C & Yaari Y (2004). KCNQ/M channels control spike afterdepolarization and burst generation in hippocampal neurons. *J Neurosci* **24**, 4614–4624.

Acknowledgements

This work was supported by the German–Israeli collaborative research programme of the Bundesministerium für Bildung und Forschung (BMBF) and the Ministry of Science (MOS), the Deutsche Forschungsgemeinschaft (SFB TR3), the Niedersachsen Foundation and the Henri J and Erna D. Leir Chair for Research in Neurodegenerative Diseases.